

Mimicking a Kerrlike medium in the dispersive regime of second-harmonic generation

A. B. Klimov

*Departamento de Física, Universidad de Guadalajara, Revolución 1500,
44420 Guadalajara, Jalisco, Mexico*

L. L. Sánchez-Soto and J. Delgado

*Departamento de Óptica, Facultad de Ciencias Físicas, Universidad Complutense,
28040 Madrid, Spain*

Abstract

We find an effective Hamiltonian describing the process of second-harmonic generation in the far-off resonant limit. We show that the dynamics of the fundamental mode is governed by a Kerrlike Hamiltonian. Some dynamical consequences are examined.

PACS number(s): 03.65.Bz, 42.50.Ct, 42.50.Vk, 42.65.Ky

Section: Quantum Optics

1 Introduction

The superposition principle plays an essential role in understanding the conceptual foundations of quantum mechanics. Stated in physical terms, it assures that we cannot speak of an objective state of a system prior to a measurement. In fact, one should admit that the system may be described as a superposition of macroscopically (or mesoscopically) distinct states, often known as Schrödinger cat states [1].

Therefore, the methods for the generation of such superposition states are of fundamental interest. Among other systems, vibrating molecules [2] or crystals [3], trapped ions [4], and Bose condensates [5] have been proposed as candidates for doing the task. In fact, mesoscopic Schrödinger cat states for the vibrational motion of ion traps have been experimental realized [6].

The issue of generating optical Schrödinger cats (namely, superpositions of distinguishable states of the electromagnetic field) has attracted as well a great deal of attention [7]. For example, Brune *et al* [8] have shown that the conditional measurement on atoms exiting a high- Q cavity may force the radiation inside the cavity to be in a catlike state. The same basic concept of conditional measurement has also been suggested for entangled states [9], nonlinear birefringence [10], or self-Kerr phase modulation [11]. The state collapse due to photodetection has also been suggested as a source of cat states [12].

The Kerr effect provides a nonlinearity of particular interest for generating field cat states [13]. Apart from their intrinsic simplicity, Kerr-based schemes have the specific advantage of not relying on conditional measurements. However, the realistic values of Kerr coefficients are quite small, thus requiring a large interaction length. Then, losses become significant and may destroy the very delicate quantum superpositions. In short, although very appealing from the physical viewpoint, Kerr schemes are not generally considered to be realistic. In spite of this belief, there has been a very recent proposal of generating a Kerr *kitten* that serves as a quantum seed for suitable amplification [14], that could become fully feasible.

On the other hand, it should be noted that perhaps the simplest nonlinear optical process is second-harmonic generation, which in addition exhibits a rich spectrum of nonclassical features. Considerable attention has been paid to issues such as photon antibunching, squeezing, or collapses and revivals [15]. However, the generation of Schrödinger cat states has gone almost unnoticed. Perhaps, a relevant exception is the work of Nikitin and Masalov [16], showing that, at resonance, the quantum state of the fundamental mode evolves into a superposition of two macroscopically distinguishable states. This point may be considered as well rather unrealistic, because the stringent experimental constraints of having perfect phase matching and low decoherence could be rather difficult to attain.

In this paper we pursue the dispersive limit of second-harmonic generation, which seems to be almost ignored in the literature. At this respect, our main result is to show that, for detunings large enough, the dynamics can be described in terms of an effective Hamiltonian essentially identical to that governing the propagation of the fundamental mode in a Kerr medium.

Apart from its intrinsic interest, such an identification could be more than an academic curiosity: second-harmonic generation is, for a variety of reasons [17], more robust than the Kerr effect as for noise-limiting factors. In consequence, this scheme could be an experimentally feasible proposal to generate the yearned optical cat states.

2 Dynamics of second-harmonic generation in the dispersive limit

Second-harmonic generation is usually described (without assuming perfect resonance) by the following model Hamiltonian (in units $\hbar = 1$)

$$H = H_0 + H_{\text{int}} = \omega_a a^\dagger a + \omega_b b^\dagger b + g(a^2 b^\dagger + a^\dagger 2 b), \quad (1)$$

where a (a^\dagger) and b (b^\dagger) are the annihilation (creation) operators of the fundamental mode of frequency ω_a and of the second-harmonic mode of frequency ω_b , respectively. When perfect matching conditions occurs, they satisfy $\omega_b = 2\omega_a$. The constant g , describing phenomenologically the coupling between both modes, can be always chosen as real.

Classically the above problem admits an exact solution, leading to the possibility of the energy being transferred completely into the second-harmonic mode [18]. Unfortunately, the corresponding quantum dynamics is a touchy business, though different algebraic, semiclassical, and numerical approaches have been developed (for pertinent literature on these approximations see Ref. [19]).

By noting that the Hamiltonian (1) admits the constant of motion

$$N = a^\dagger a + 2b^\dagger b, \quad (2)$$

it can be recast in the following simple form

$$\begin{aligned} H_0 &= \frac{\omega_b + \omega_a}{3} N, \\ H_{\text{int}} &= \frac{\Delta}{3} (b^\dagger b - a^\dagger a) + g(a^2 b^\dagger + a^\dagger 2 b), \end{aligned} \quad (3)$$

where

$$\Delta = \omega_b - 2\omega_a \quad (4)$$

is the detuning.

It is straightforward to check that

$$[H_0, H_{\text{int}}] = 0, \quad (5)$$

so both H_0 and H_{int} are constants of motion. Since H_0 determines the total energy stored in both modes, which is conserved, we can factor out $\exp(-iH_0t)$ from the evolution operator and drop it altogether.

In order to examine the quantum evolution we shall use a standard numerical approach developed by Tanaš and coworkers [20] starting from the original one of Walls and Barakat [21]. First, we consider the case of perfect resonance and we take the typical experimental conditions; namely, the fundamental mode in a coherent state with an average number of photons \bar{n}_a and the harmonic mode in the vacuum.

For definiteness, we shall analyze the quantum state by computing the Q function. In figure 1 we have plotted a gray-scale contour map of this distribution $Q(\alpha)$ for the fundamental mode with $\bar{n}_a = 10$, and for different values of the dimensionless time $\tau = gt\sqrt{2\bar{n}_a}$. Results are in complete agreement with the previous work by Nikitin and Masalov [16]: at the beginning of the interaction ($\tau < 2$) the uncertainty contour turns to an ellipse, whose long axis is perpendicular to the field vector (so the state is squeezed in amplitude). Further interaction ($\tau \simeq 4$) results in a bifurcation of the Q distribution and the formation of a superposition of two macroscopically distinguishable states. Subsequent development ($\tau > 5$) destroys this state as well.

Next, we consider the case when some mismatch is present. The previous numerical procedure is still valid, but one must take care of the diagonal extra terms introduced by the detuning. To check how the detuning affects the cats, in figure 2 we have plotted the contours of the Q function at $\tau = 4$, when the cat should appear, for different values of the dimensionless detuning Δ/g . One easily notices that the cat becomes more and more blurred as the detuning increases, until Δ/g is so large and the process is so inefficient that the fundamental mode does not feel any appreciable interaction and the cat is lost. Moreover, we have found no numerical evidence of any further cat for other times around $\tau = 4$.

This is a reasonable result from the physical viewpoint, since one could expect some kind of continuity. However, it differs from the numerical computations of Nikitin and Masalov [16], who find that the cat disappears as soon as some detuning is present, irrespectively the smaller this detuning is. The reason is the way they deal with the off-resonant situation: following a classical argument, they assume that the presence of detuning translates into the fact that the coupling constant has the time dependence $g = |g| \exp[(n_a - n_b)\omega t]$, where n_a and n_b are the refractive indices of the medium at the frequencies ω_a and ω_b . In such a way, the interaction Hamiltonian H_{int} becomes time dependent and the numerical method becomes rather complicated, at difference of what happens with our very simple model.

From now on, we shall be interested in the dispersive limit of the model governed by the Hamiltonian (1). In other words, we shall consider the situation when

$$|\Delta| \gg g(\bar{n}_a + 1)(\bar{n}_b + 1), \quad (6)$$

where \bar{n}_a and \bar{n}_b denote the average photon numbers in the modes a and b , respectively. It is worth emphasizing that this is a limit physically realizable in practice [22]. Now, the essential point is that g/Δ can be considered as a small parameter and, according to the method developed in Ref. [23], we can apply a unitary transformation to the interaction Hamiltonian (3)

$$H_{\text{eff}} = U H_{\text{int}} U^\dagger, \quad (7)$$

where

$$U = \exp \left[\frac{g}{\Delta} (a^2 b^\dagger - a^{\dagger 2} b) \right]. \quad (8)$$

To gain a deeper insight into the physical ideas underlying the method we can introduce the operators

$$\begin{aligned} X_+ &= b^\dagger a^2, & X_- &= a^{\dagger 2} b, \\ X_3 &= \frac{1}{3}(b^\dagger b - a^\dagger a), \end{aligned} \quad (9)$$

that satisfy the commutation relations

$$\begin{aligned} [X_3, X_\pm] &= \pm X_\pm, \\ [X_+, X_-] &= P(X_3), \end{aligned} \quad (10)$$

where P refers to a quadratic polynomial function of the diagonal operator X_3 . Then, while the first relation is the same as the corresponding one for the standard $\text{su}(2)$ algebra, the second one defines what is called a nonlinear or polynomial deformation of $\text{su}(2)$ [23]. From this viewpoint, the transformation (8) can be recast as

$$U = \exp \left[\frac{g}{\Delta} (X_+ - X_-) \right]. \quad (11)$$

For $\text{su}(2)$ operators this would be simply a rotation. Here, it represents a small nonlinear rotation with the parameters chosen in such a way so as to

cancel [up to order $(g/\Delta)^2$] the nondiagonal terms appearing in the transformed Hamiltonian. Moreover, its unitary character ensures that H_{eff} has the same spectrum as H_{int} (so they are physically equivalent). In consequence, by expanding Eq. (7) in a power series and keeping terms up to the order $(g/\Delta)^2$, we finally get

$$H_{\text{eff}} = \frac{\Delta}{3}(b^\dagger b - a^\dagger a) - \lambda [4b^\dagger b a^\dagger a - (a^\dagger a)^2], \quad (12)$$

with

$$\lambda = \frac{g^2}{\Delta}. \quad (13)$$

The effective Hamiltonian (12) describes the dispersive evolution of the fields, but the essential point is that it is diagonal, which implies that there is no population transfer between the modes (as it is expected in the far-off resonant limit). The first term in Eq. (12) does not affect the dynamics and just leads to a rapid oscillation of the wavefunction. It is worth noting that the small rotation generated by the transformation (8) just adds small corrections of order g/Δ to the physical observables and, thus, the state vector need not to be transformed.

Now, it is easy to find evolution of the density matrix of the fundamental mode. When the harmonic mode is initially in the vacuum, the two terms containing $b^\dagger b$ in Eq. (12) do not contribute. In addition, the linear term in $a^\dagger a$ lead just to a *c*-number phase shift and can be also omitted. Then, the effective Hamiltonian reduces to

$$H_K = \lambda(a^\dagger a)^2, \quad (14)$$

which is nothing but the interaction Hamiltonian that governs the state evolution of the single-mode field a in a Kerr medium. Then, the evolution is factorized all the times (in the frame of this approximation) and, in consequence, starting from a coherent state in mode a , one will recover M copies of this initial state at times $\lambda t = \pi/M$ [13]. In particular, for $\lambda t = \pi/2$ the density matrix of the fundamental mode becomes

$$\rho_a(\pi/2\lambda) = |\psi_c\rangle_a a \langle \psi_c|, \quad (15)$$

where $|\psi_c\rangle_a$ is a superposition of two coherent states with opposite phases; i.e.,

$$|\psi_c\rangle_a = \frac{1}{\sqrt{2}} [e^{i\pi/4}|\alpha\rangle_a + e^{-i\pi/4}|-\alpha\rangle_a]. \quad (16)$$

To check these predictions we have numerically calculated the Q function from the exact Hamiltonian (3) at the time $t = \pi/(2\lambda)$. The initial coherent state in mode a has $\bar{n}_a = 10$ and we have assumed a detuning $\Delta/g = 50$, which is enough to guarantee the validity of our approximation (6). In figure 3 we have plotted the results of the computation, showing an apparent excellent agreement with the expected cat. However, the Q function by itself is not very suitable to distinguish between coherent and incoherent superpositions. To further confirm the coherent behavior we have considered the fidelity

$$\mathcal{F}(t) = {}_a\langle\psi_c|\rho(t)|\psi_c\rangle_a \quad (17)$$

between the ideal two-component cat density matrix and the state coming from realistic evolution. In figure 4 we have plotted the resulting fidelity as a function of the rescaled time gt for $\Delta/g = 50$. We can see the presence of small peaks corresponding to the presence of M -component catlike states, as well as the strong peak at the time $\lambda t = \pi/2$ predicted by our theory when $M = 2$.

When the initial state of the harmonic mode is in a superposition of number states instead of the vacuum, the dynamics of the fundamental mode is drastically affected. For simplicity, we shall take an initial coherent state in both modes, namely, $|\alpha\rangle_a \otimes |\beta\rangle_b$. Then, we obtain for the density matrix of the fundamental mode the following expression

$$\begin{aligned} \rho_a(t) &= e^{-|\alpha|^2} \sum_{n,m}^{\infty} e^{it\lambda(n^2-m^2)} \exp \left[|\beta|^2 \left(1 - e^{-4i\lambda t(n-m)} \right) \right] \\ &\times \frac{\alpha^n \alpha^{*m}}{\sqrt{n!m!}} |n\rangle_a {}_a\langle m|. \end{aligned} \quad (18)$$

The entanglement between modes a and b is evident, as well as the fact that only when $\lambda t = \pi/2$ they become disentangled and two copies of the initial coherent state in the fundamental mode will be created. Indeed, the density matrix of the total system at such time is

$$\rho(\pi/2\lambda) = |\beta\rangle_b {}_b\langle\beta| \otimes |\psi_c\rangle_a {}_a\langle\psi_c|, \quad (19)$$

and only a two-component cat can be produced in this case, although with lesser fidelity than for the vacuum. On the contrary, when $\lambda t = \pi$, the initial coherent state is reconstructed.

Finally, some comments concerning the physical feasibility of the proposed scheme seem in order. Of course, a simple comparison of the parameters in figures 1 and 3 clearly shows that the times required for the appearance of the cat in the dispersive limit are an order of magnitude larger than in the

usual case of no detuning. The advantage of this dispersive limit is twofold: one does not need to take care about phase-matching considerations and, more important, if the process takes place in a cavity, one could expect from previous results, e.g. in cavity quantum electrodynamics [22], that the quantum features of the state may be undestroyed for large interaction times. In addition, the width of the peak appearing in the fidelity is of the order of 5 in units of gt , while the cat appearing in figure 1 disappears in much shorter times. Thus, the required time resolution in this dispersive limit is lesser than the one needed for the perfect frequency-matching case. In spite of these advantages, the required times are still so long that other decoherence factors could affect the final results.

The effective Hamiltonian (12) has the virtue of simplifying calculations that otherwise would be rather involved. To cite only an example, the squeezing properties of the fundamental mode are also affected by the initial state of the harmonic mode. For initial coherent states in both modes $|\alpha\rangle_a \otimes |\beta\rangle_b$ (for simplicity, we take α and β as real numbers) we easily get for the variance $\sigma_x^2 = \langle x^2 \rangle - \langle x \rangle^2$ of the quadrature $x = (a + a^\dagger)/\sqrt{2}$

$$\begin{aligned} \sigma_x^2(t) = & \frac{1}{2} + \alpha^2(e^{-8z^2T^2} - e^{-4z^2T^2}) \cos \Omega T \\ & - 2\alpha^2T^2(4e^{-8z^2T^2} - e^{-4z^2T^2}) \cos \Omega T \\ & - 2\alpha^2T(2e^{-8z^2T^2} - e^{-4z^2T^2}) \sin \Omega T \\ & + \alpha^2(1 - e^{-4z^2T^2}) \cos \Omega T, \end{aligned} \quad (20)$$

where $T = \lambda t \ll 1$, $z^2 = \alpha^2 + 4\beta^2$, and $\Omega = 4\alpha^2 - 8\beta^2$. Then, for sufficiently large values of β^2 squeezing in the fundamental mode disappears, according to previous numerical studies [16].

One could be tempted to extend the method to other nonlinear optical process in order to get effective Hamiltonians that are diagonal in the desired basis. In fact, the program can be carried out. For example, for third-harmonic generation one obtains, after repeating the same steps as before,

$$H_{\text{eff}} \simeq \lambda \left\{ 9b^\dagger b \left[(a^\dagger a)^2 + a^\dagger a \right] - (a^\dagger a)^3 - 6(a^\dagger a)^2 \right\}, \quad (21)$$

but now the final result contains a cubic nonlinearity and the problem is not facilitated at all.

3 Concluding remarks

What we expect to have accomplished in this paper is to present a simple model for the description of the dispersive limit of second-harmonic generation in terms of an effective Hamiltonian that is diagonal and contains Kerrlike nonlinearities. Of course, in the practice other off-resonant processes could also contribute to the third-order nonlinearity. However, our effective-Hamiltonian approach can explain (at least qualitatively) some unexpected and fascinating behaviors of the so-far unnoticed dispersive limit.

Of course, it is well known that when some interaction energy is off-resonant then, in a higher order of perturbation theory an effective interaction energy can be constructed that gives rise to resonant processes. At this respect, in Ref. [23] it has been shown how the method of small rotations can be used to tailor resonant interactions from nonresonant processes, just as demonstrated in this paper for the relevant case of the second-harmonic generation.

Finally, it is worth noting as well that the Hamiltonian (12) is similar to that obtained in Ref. [24] for the Dicke model in the large detuning limit (when the effective Hamiltonian was proportional to S_z^2).

References

- [1] E. Schrödinger, in *Quantum Theory of Measurement*, edited by J. A. Wheeler and W. H. Zurek (Princeton University Press, Princeton, NJ) p. 152.
- [2] J. Janzky, A. V. Vinogradov, T. Kobayashy, Z. Kis, Phys. Rev. A **50**, 1777 (1994)
- [3] I. A. Walmsley, M. G. Raymer, Phys. Rev. A **52**, 681 (1995)
- [4] J. J. Slosser, P. Meystre, E. M. Wright, Opt. Lett. **15**, 233 (1990)
R. L. de Matos-Filho, W. Vogel, Phys. Rev. Lett. **76**, 608 (1996)
M. M. Nieto, Phys. Lett. A **219**, 180 (1996)
- [5] J. I. Cirac, M. Lewenstein, K. Molmer, P. Zoller, Phys. Rev. A **57**, 1208 (1998)
- [6] C. Monroe, D. M. Meekhof, B. E. King, D. J. Wineland, Science **272**, 1131 (1996)
D. M. Meekhof, C. Monroe, B. E. King, W. M. Itano, D. J. Wineland, Phys. Rev. Lett. **76**, 1796 (1996)
D. Leibfried, D. M. Meekhof, B. E. King, C. Monroe, W. M. Itano, D. J. Wineland, Phys. Rev. Lett. **77**, 4281 (1996)

- D. J. Wineland, C. Monroe, D. M. Meekhof, D. Leibfried, W. M. Itano, J. C. Bergquist, D. Berkeland, J. J. Bollinger, J. Miller, Proc. Roy. Soc. A **454**, 411 (1998)
- [7] V. V. Dodonov, I. A. Malkin, V. I. Man'ko, Physica **72**, 4281 (1974)
M. Hillery, Phys. Rev. A **36**, 3796 (1987)
G. C. Gerry, Opt. Commun. **63**, 278 (1987)
R. Lynch, Opt. Commun. **67**, 67 (1988)
W. Schleich, M. Pernigo, F. Le Kien, Phys. Rev. A **44**, 2172 (1991)
V. Bužek, H. Moya-Cessa, P. L. Knight, S. J. D. Phoenix, Phys. Rev. A **45**, 8190 (1992)
- [8] M. Brune, S. Haroche, J. M. Raimond, L. Davidovich, N. Zagury, Phys. Rev. A **45**, 5193 (1992)
L. Davidovich, M. Brune, J. M. Raimond, S. Haroche, Phys. Rev. A **53**, 1295 (1996)
M. Brune, E. Hagley, J. Dreyer, X. Maître, A. Maali, C. Wunderlich, J. M. Raimond, S. Haroche, Phys. Rev. Lett. **77**, 4887 (1996)
- [9] S. Song, C. M. Caves, B. Yurke, Phys. Rev. A **41**, 5261 (1990)
B. Yurke, W. P. Schleich, D. F. Walls, Phys. Rev. A **42**, 1703 (1990)
P. Tombesi, D. Vitali, Phys. Rev. Lett. **77**, 411 (1996)
M. Dakna, T. Anhut, T. Opatrny, L. Knoll, D. G. Welsch, Phys. Rev. A **55**, 3184 (1997)
- [10] A. Mecozzi, P. Tombesi, Phys. Rev. Lett. **58**, 1055 (1987)
- [11] B. Yurke, D. Stoler, Phys. Rev. Lett. **57**, 13 (1986)
S. D. Du, S. Gong, Z. Z. Xu, L. W. Zhou, C. D. Gong, Opt. Commun. **138**, 193 (1997)
- [12] M. Ban, J. Mod. Opt. **43**, 1281 (1996)
M. Ban, Phys. Lett. A **233**, 284 (1997)
A. Luis, L. L. Sánchez-Soto, Phys. Lett. A **244**, 211 (1998)
- [13] M. Kitagawa, Y. Yamamoto, Phys. Rev. A **34**, 3974 (1986)
G. S. Milburn, Phys. Rev. A **33**, 674 (1986)
R. Tanaś, Ts. Gantsog, A. Miranowicz, S. Kielich, J. Opt. Soc. Am. B **8**, 1576 (1991)
R. Tara, G. S. Agarwal, S. Chaturvedi, Phys. Rev. A **47**, 5024 (1993)
G. V. Varada, G. S. Agarwal, Phys. Rev. A **48**, 4062 (1993)
- [14] M. G. A. Paris, J. Opt. B: Quantum Semiclass. Opt. **1**, 662 (1999)

- [15] M. Kozierovski, R. Tanaś, Opt. Commun. **21**, 229 (1977)
L. Mandel, Opt. Commun. **42**, 437 (1982)
L. Wu, H. J. Kimble, J. L. Hall, H. Wu, Phys. Rev. Lett. **57**, 2520 (1986)
G. Drobný, I. Jex, Phys. Rev. A **46**, 499 (1992)
G. Drobný, I. Jex, V. Bužek, Phys. Rev. A **48**, 569 (1993)
- [16] S. P. Nikitin, A. V. Masalov, Quantum Opt. **3**, 105 (1991)
- [17] A. G. White, P. K. Lam, D. E. McClelland, H-A. Bachor, W.J. Munro, J. Opt. B: Quantum Semiclass. Opt. **2**, 553 (2000)
- [18] N. Bloembergen, *Nonlinear Optics* (McGraw-Hill, New York, 1972)
- [19] R. F. Alvarez-Estrada, A. Gómez-Nicola, L. L. Sánchez-Soto, A. Luis, J. Phys. A **28**, 3439 (1995)
G. Alvarez, R. F. Alvarez-Estrada, J. Phys. A **28**, 5767 (1995)
- [20] R. Tanaś, Ts. Gantsog, R. Zawodny, Quantum Opt. **3**, 221 (1991)
- [21] D. F. Walls, R. Barakat, Phys. Rev. A **1**, 446 (1970)
- [22] M. Brune, E. Hagley, J. Dreyer, X. Maître, A. Maali, C. Wunderlich, J. M. Raimond, S. Haroche, Phys. Rev. Lett. **77**, 4887 (1996)
- [23] A. B. Klimov, L. L. Sánchez-Soto, Phys. Rev. A **61**, 063802 (2000)
- [24] G. S. Agarwal, R.R.Puri, R.P.Singh, Phys. Rev. A **56**, 2249 (1997)

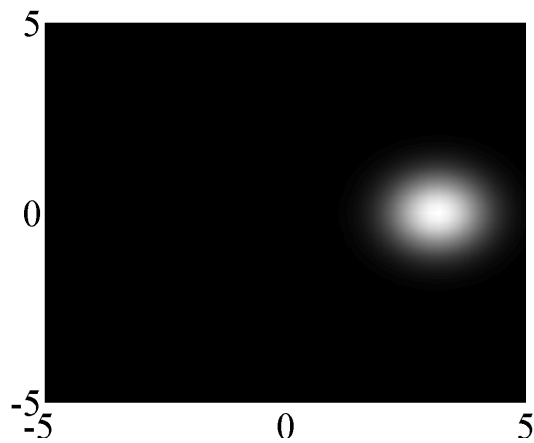
Fig. 1. Gray-level contour plot of the quasiprobability distribution $Q(\alpha)$ of the fundamental mode (with perfect frequency matching) at different times $\tau = gt\sqrt{2\bar{n}_a}$. Initially, the fundamental mode is in a coherent state with $\bar{n}_a = 10$ and the harmonic mode is in the vacuum. In all the cases in the horizontal axis we plot $\text{Re } \alpha$ and in the vertical we plot $\text{Im } \alpha$.

Fig. 2. Gray-level contour plot of the quasiprobability distribution $Q(\alpha)$ of the fundamental mode for the same initial state as in figure 1 calculated for $\tau = 4$ at different values of Δ/g .

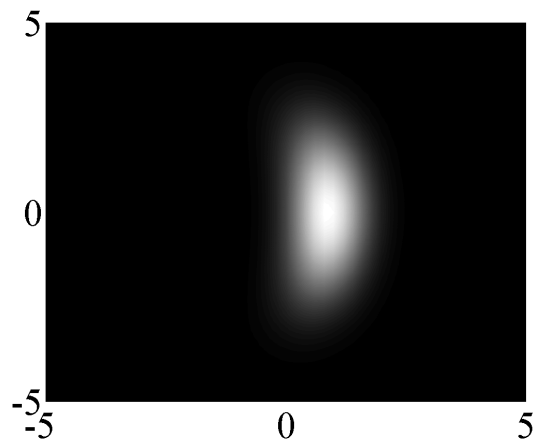
Fig. 3. Q function and the corresponding contour plot of the fundamental mode (initially, the fundamental mode is in a coherent state with $\bar{n}_a = 10$ and the harmonic mode is in the vacuum) with a detuning of $\Delta/g = 50$. The function has been calculated from the exact interaction Hamiltonian (3) at $\lambda t = \pi/2$.

Fig. 4. Fidelity of the fundamental mode respect to the ideal cat state as a function of the rescaled time gt . The state evolution has been calculated from the exact interaction Hamiltonian (3). The initial state is as in figure 3 with the same detuning $\Delta/g = 50$. The main peak appears at the time $\lambda t = \pi/2$ predicted by the theory.

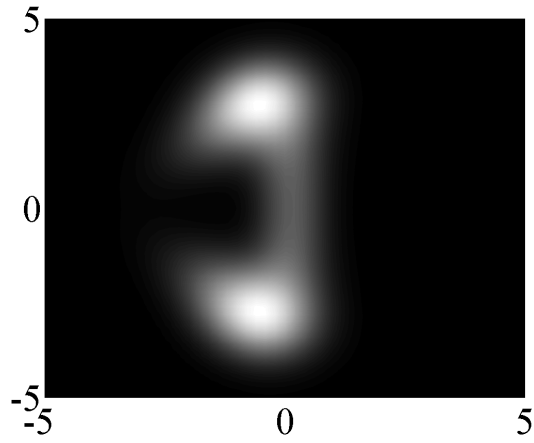
$\tau=0$



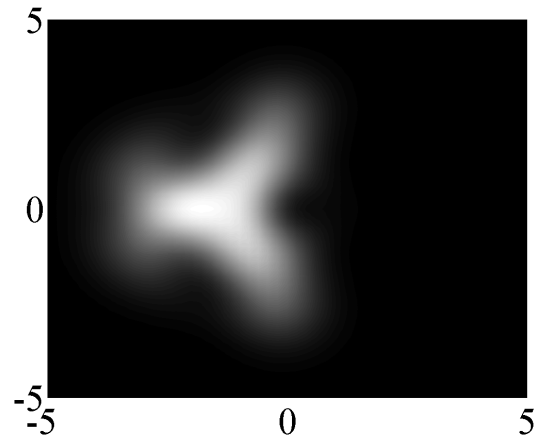
$\tau=2$



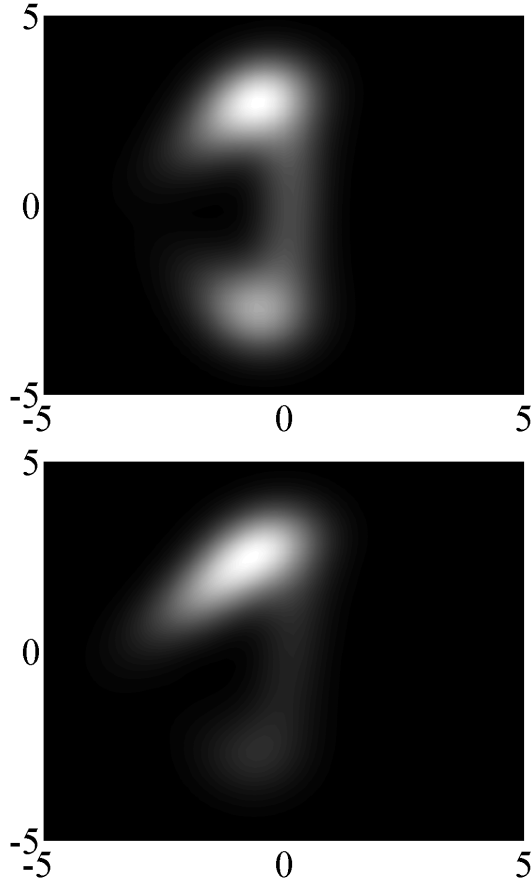
$\tau=4$



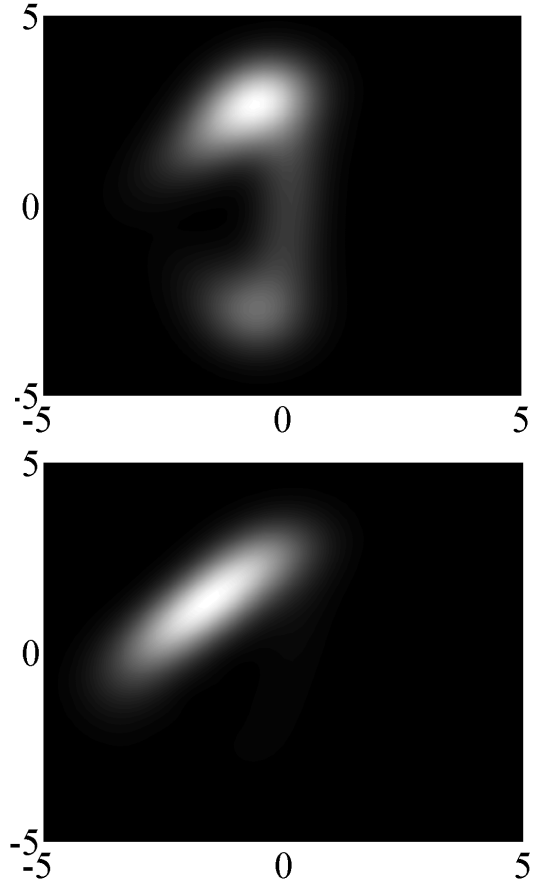
$\tau=6$



$\Delta/g=50$



$\Delta/g=100$



$\Delta/g=200$

$\Delta/g=400$

